THE JOURNAL OF COMPARATIVE NEUROLOGY 495:497–510 (2006)

Development of γ-Aminobutyric Acidergic Synapses in Cultured Hippocampal Neurons

CATHERINE CROFT SWANWICK,[1] NAMITA R. MURTHY,[2] ZAKARIA MTCHEDLISHVILI,[3] WERNER SIEGHART,[4] AND JAIDEEP KAPUR[1,3]*
[1]Neuroscience Graduate Program, University of Virginia, Charlottesville, Virginia 22908
[2]College of Arts and Sciences, University of Virginia, Charlottesville, Virginia 22908
[3]Department of Neurology, University of Virginia, Charlottesville, Virginia 22908
[4]Center for Brain Research, Medical University of Vienna, A1090 Vienna, Austria

ABSTRACT

The formation and maturation of γ-aminobutyric acid (GABA)-ergic synapses was studied in cultured hippocampal pyramidal neurons by both performing immunocytochemistry for GABAergic markers and recording miniature inhibitory postsynaptic currents (mIPSCs). Nascent GABAergic synapses appeared between 3 and 8 days in vitro (DIV), with $GABA_A$ receptor subunit clusters appearing first, followed by GAD-65 puncta, then functional synapses. The number of GABAergic synapses increased from 7 to 14 DIV, with a corresponding increase in frequency of mIPSCs. Moreover, these new GABAergic synapses formed on neuronal processes farther from the soma, contributing to decreased mIPSC amplitude and slowed mIPSC 19–90% rise time. The mIPSC decay quickened from 7 to 14 DIV, with a parallel change in the distribution of the α5 subunit from diffuse expression at 7 DIV to clustered expression at 14 DIV. These α5 clusters were mostly extrasynaptic. The α1 subunit was expressed as clusters in none of the neurons at 7 DIV, in 20% at 14 DIV, and in 80% at 21 DIV. Most of these α1 clusters were expressed at GABAergic synapses. In addition, puncta of GABA transporter 1 (GAT-1) were localized to GABAergic synapses at 14 DIV but were not expressed at 7 DIV. These studies demonstrate that mIPSCs appear after pre- and postsynaptic elements are in place. Furthermore, the process of maturation of GABAergic synapses involves increased synapse formation at distal processes, expression of new $GABA_A$ receptor subunits, and GAT-1 expression at synapses; these changes are reflected in altered frequency, kinetics, and drug sensitivity of mIPSCs. J. Comp. Neurol. 495:497–510, 2006.

Indexing terms: synaptogenesis; $GABA_A$ receptor; GABA transporter; mIPSC

Three basic stages of synaptogenesis have been described: 1) initial contact between presynaptic and postsynaptic elements, 2) maturation of the synapse, and 3) emergence of adult isoforms (Sanes et al., 2000). Most studies of synaptogenesis have concentrated on the neuromuscular junction and glutamatergic synapses (Sanes and Lichtman, 2001; Goda and Davis, 2003). Although the formation and organization of γ-aminobutyric acid (GABA)-ergic synapses are thought generally to follow the same process (Moss and Smart, 2001; Meier, 2003), the development of GABAergic synapses has not been fully characterized.

Nascent GABAergic synapses should contain both presynaptic and postsynaptic elements, as well as produce synaptic transmission (Ahmari and Smith, 2002). Previous studies demonstrated that $GABA_A$ receptors formed clusters before presynaptic terminals emerged (Scotti and Reuter, 2001), and this clustering occurred in the absence

Grant sponsor: National Institutes of Health–National Institute of Neurological Disorders and Stroke; Grant number: F31 NS 43831 (to C.C.S.); Grant number: R01 NS 040337 (to J.K.); Grant number: RO1 NS 44370 (to J.K.); Grant sponsor: the Austrian Science Fund; Grant number: FWF-P15165 (to W.S.).

*Correspondence to: Jaideep Kapur, Department of Neurology, Box 800394, University of Virginia-HSC, Charlottesville, VA 22908.
E-mail: jk8t@virginia.edu

Received 29 March 2005; Revised 9 June 2005; Accepted 24 October 2005
DOI 10.1002/cne.20897
Published online in Wiley InterScience (www.interscience.wiley.com).

of scaffolding proteins and GABA release (Craig et al., 1994; Rao et al., 2000; Scotti and Reuter, 2001; Christie et al., 2002). Also, during maturation, $GABA_A$ receptors became selectively clustered across from terminals that release the neurotransmitter GABA (Craig et al., 1994). However, these studies did not specify the relationship of GABAergic protein expression and the onset of GABAergic synaptic transmission.

Once GABAergic synapses are formed, they undergo profound maturational changes in both composition and function. Molecular changes may occur at the presynaptic terminal, within $GABA_A$ receptor subunit composition or GABA transporter subtype. A well-studied locus of alteration is the composition of $GABA_A$ receptor subunits (Killisch et al., 1991; Laurie et al., 1992; Brooks-Kayal et al., 1998). The $GABA_A$ receptor channel is composed of five subunits derived from eight subfamilies of subunit genes. Each subunit gene family has multiple members (α has six, β has four, γ has three, ρ has three, and δ, ε, π, and θ have one each). There is a regionally distinct progression in cellular expression patterns of $GABA_A$ receptor subunits during postnatal development. However, few studies correlate the maturation of synapses with functional changes in transmission.

Functionally, the kinetics of $GABA_A$ receptor-mediated synaptic currents change during development. Changes in the frequency amplitude and decay of miniature inhibitory postsynaptic currents (mIPSCs) occur during postnatal development of various brain regions, including the cerebellum (Tia et al., 1996; Vicini et al., 2001), hippocampus (Cohen et al., 2000), thalamus (Okada et al., 2000), superior colliculus (Juttner et al., 2001), and brainstem (Sanes et al., 1993). However, the temporal relationship of developmental changes in the kinetics of mIPSCs to the composition of GABAergic synapses has not been studied. Here we explored the relationship between the molecular and the functional maturation of GABAergic synapses in cultured hippocampal neurons prepared by using methods previously established (Fletcher et al., 1991; Rao et al., 2000; Mangan and Kapur, 2004) that provide the advantages of accessibility to and visibility of individual synapses.

MATERIALS AND METHODS

Cell culture

Neuronal hippocampal/glial cocultures were prepared from 18-day embryonic rats as previously described (Goslin et al., 1998). Glial cell cultures were prepared 10 days prior to coculturing with hippocampal neurons when, in a laminar flow hood, neonatal Sprague-Dawley rat pups were decapitated after being placed on ice for 2–3 minutes. Hippocampal neuron cultures were prepared later, when Sprague-Dawley rat fetuses were removed from the pregnant mother after she was anesthetized with halothane. Fetuses were then decapitated and brains removed. These methods were approved by the University of Virginia Animal Care and Use Committee and conform to NIH guidelines. Briefly, neurons were isolated by trypsin treatment, triturated, and plated on poly-L-lysine-coated glass coverslips in minimum essential medium (MEM) with 15% horse serum at a density of 10,000–100,000 cells/35 mm^2. After attachment of cells, coverslips were transferred, and neurons grew over a glial cell monolayer in serum-free MEM with N2 supplements. The population of neurons in culture consisted primarily of pyramidal neurons, which could be distinguished morphologically from GABAergic interneurons that composed approximately 6% of cells (Benson et al., 1994). Neurons were analyzed 1–21 days after plating. However, because expression of presynaptic and postsynaptic markers remained relatively constant from 14 to 21 DIV, only data from 14 DIV are presented.

Immunocytochemistry

Single-label and double-label immunocytochemistry for presynaptic and postsynaptic GABAergic markers was performed according to methods previously described (Swanwick et al., 2004). The γ2 and β2/3 subunits of the $GABA_A$ receptor were used as postsynaptic markers, because the γ2 subunit is required for synaptic targeting of $GABA_A$ receptors (Essrich et al., 1998), and β2/3 is one of the most abundant subunits of $GABA_A$ receptors in the brain (McKernan and Whiting, 1996). The 65-kDa isoform of glutamic acid decarboxylase (GAD-65), the synthetic enzyme for GABA, was used as a presynaptic marker. Two forms of GAD exist: GAD-65 and GAD-67 (Erlander et al., 1991). All GABAergic neurons make both isoforms, but GAD-65 immunoreactivity is concentrated in synapses, whereas GAD-67 immunoreactivity is prominent in cell bodies (Kaufman et al., 1991; Dupuy and Houser, 1996). All measurements were performed in pyramidal neurons that were visually identified based on morphology (Benson et al., 1994).

Primary antibodies. All primary antibodies were diluted in 0.1 M phosphate-buffered saline (PBS; pH 7.1) containing 2% normal goat serum. The specificity of each antibody was verified by the lack of staining after the omission of the primary antibody or serial dilution.

A mouse monoclonal antibody recognized amino acids 1–3 common to the β2 and β3 subunits of the $GABA_A$ receptor (clone 62-3G1, 2 μg/ml, Upstate, Lake Placid, NY; No. 05-474). This antibody visualizes two bands on a Western blot, 55 kDa (β2) and 57 kDa (β3), and immunoreactivity to these bands was specifically blocked by the corresponding peptide (Li and De Blas, 1997). A rabbit antibody recognized the γ2 subunit of the $GABA_A$ receptor (amino acids 319–366, 2 μg/ml). Immunoblotting using this antibody shows a band of 45–49 kDa (Mossier et al., 1994; Sun et al., 2004) and adsorption of the antibody blocked its detection (Togel et al., 1994). Immunocytochemical characterization of this antibody has been performed previously (Sperk et al., 1997; Nusser et al., 1998; Sun et al., 2004).

A mouse monoclonal antibody recognized GAD-65 (GAD-6 clone, 1 μg/ml; Chemicon, Temecula, CA; No. MAB351). This antibody binds to a single band of 65 kDa on a Western blot, and its specificity was verified through adsorption (Chang and Gottlieb, 1988). A rabbit antibody raised against GAD-65 was also used (GAD-6 clone, 1:1,000, Chemicon; No. AB5082). It also recognized a band of 65 kDa on a Western blot whose detection was blocked by preadsorption with the peptide and that has been immunocytochemically characterized (Mi et al., 2002).

A rabbit antibody recognized the α1 subunit of the $GABA_A$ receptor (amino acids 1–16, 1.5 μg/ml, Alomone Labs, Jerusalem, Israel; No. AGA-001). This antibody reveals a single band of ~50 kDa on a Western blot (Sun et al., 2004) that was blocked by preadsorption with the synthetic peptide. A rabbit antibody recognized the α2

subunit of the $GABA_A$ receptor (C-terminal peptide, 1:2,000; Abcam Inc., Cambridge, MA; No. ab8342). On a Western blot, this antibody (1:2,500) revealed a single band of 53 kDa (C. Sun and J. Kapur, unpublished observations), and its specificity has been characterized previously (Poulter et al., 1999; Brandon et al., 2000). A rabbit antibody recognized the α4 subunit of the $GABA_A$ receptor (amino acids 1–14, 5 μg/ml). A 67-kDa band is visible with use of this antibody for Western blotting (Kern and Sieghart, 1994; Bencsits et al., 1999, Sun et al., 2004), and this band is not detectable after preadsorption with the synthetic peptide (Kern and Sieghart, 1994). Moreover, this antibody has previously been characterized immunocytochemically (Sperk et al., 1997; Sun et al., 2004; Mangan et al., 2005). A rabbit antibody recognized the α5 subunit of the $GABA_A$ receptor (amino acids 337–388, 5 μg/ml). This antibody detects a single band of 47 kDa on a Western blot (Sieghart et al., 1993; S.A. Trotter and J. Kapur, unpublished observations), and adsorption of the antibody blocked this detection (Sieghart et al., 1993). A rabbit antibody recognized the δ subunit of the $GABA_A$ receptor (amino acids 1–44, 5 μg/ml). A band of ~53–57 kDA is visible on Western blotting (Sperk et al., 1997; Sun et al., 2004). Immunocytochemical characterization of this antibody has been performed previously (Sperk et al., 1997; Nusser et al., 1998; Sun et al., 2004; Mangan et al., 2005). Also, no specific labeling was evident in δ subunit-deficient mice (Peng et al., 2002).

A rabbit antibody recognized GABA transporter 1 (amino acids 588–599, 1:500; Chemicon; No. AB1570W). This antibody detects a single band of 67 kDa on a Western blot (Vitellaro-Zuccarello et al., 2003), and this immunoreactivity was prevented by preadsorption with the synthetic peptide (Ribak et al., 1996). A rabbit antibody recognized GABA transporter 3 (amino acids 607–627, 1:500; Chemicon; No. AB1574). A single band of 70 kDa is visible with use of this antibody for Western blotting (Vitellaro-Zuccarello et al., 2003), and this was also prevented by preadsorption with the synthetic peptide (Ribak et al., 1996).

Secondary antibodies. Secondary antibodies included goat anti-mouse IgG or goat anti-rabbit IgG conjugated with Alexa 488 and Alexa 594 fluorochromes (4 μg/ml; Molecular Probes, Eugene, OR). All secondary antibodies were diluted in 0.1 M PBS (pH 7.1) containing 2% normal goat serum.

Image acquisition and analysis

Pyramidal neurons were randomly selected for immunocytochemical analysis from two or more cultures. Fluorescent images of cells were captured on a CoolSnap cf CCD camera (Roper Scientific Photometrics) mounted on an Eclipse TE200 fluorescent microscope (Nikon) driven by Metamorph imaging software (Universal Imaging Corp., Downington, PA). High-resolution digital images of each fluorochrome were acquired with a ×60/1.4 NA lens. Brightness and contrast of fluorescent images were adjusted in Metamorph software so that only punctate fluorescence, but no weak diffuse background labeling, was visible.

Definition of puncta/clusters. For cluster count, size, and colocalization, thresholds were set to detect punctate fluorescence that was twofold higher than diffuse background labeling. Number of clusters was then measured. Aggregations of two or more pixels were selected as clusters, which corresponded to ≥0.15 μm diameter at ×60 magnification, as determined by 1-μm-diameter fluorescent microspheres. Images were also visually inspected to eliminate the soma, fused puncta, or obvious debris from being selected for analysis. Controls lacking primary antibody showed nonspecific labeling that could appear as granular clusters of fewer than seven pixels (<0.54 μm diameter), so, if average cluster size was below seven pixels, cluster number was recorded as 0. Because of the fluorescent intensity of the soma, only clusters on processes were quantitated for all neurons. Number of clusters was quantified per field after a single neuron was centered in the visual field.

Analysis of colocalization. A binary image was created from each thresholded image. Binary images were then added together to display overlapping puncta. Number of colocalized puncta or clusters was then measured. Data on number, size, and colocalization of puncta or clusters were analyzed in GraphPad Prism 4.0 (GraphPad, San Diego, CA). All values are reported as mean ± SEM. Values compared between 7 and 14 DIV were analyzed by using a two-tailed Student's *t*-test with a significance value of $P < 0.05$. Values for the size of β2/3 and γ2 clusters compared between 3, 7, and 14 DIV were evaluated by using a one-way ANOVA, followed by Bonferroni's multiple-comparison test.

Quantification of ×20 fields. To analyze the percentage of neurons expressing GAD-65 puncta from 3–8 DIV, images were obtained by using a ×20 objective. Random fields in the center, top, bottom, left, and right regions of the slide were chosen at each age from two or more cultures. The number of neurons expressing GAD-65 puncta was divided by the number of total neurons in the field to obtain the percentage of neurons with GAD-65 puncta.

Photomicrograph production. Images were saved as eight-bit TIFF files and opened in Adobe Photoshop 6.0 (Adobe, San Jose, CA), where overall brightness was increased for final production.

mIPSC recording

Synaptic currents mediated by the $GABA_A$ receptor were recorded from visually identified hippocampal pyramidal neurons by using the whole-cell patch clamp method as described in the previously (Hamill et al., 1981; Mangan and Kapur, 2004). Membrane properties of these neurons at 14 DIV were also previously characterized (Mangan and Kapur, 2004). mIPSCs were recorded by blocking both excitatory neurotransmission and action potentials: glutamate receptor-mediated synaptic currents were blocked by using 50 μM D(−)-2-amino-5-phosphonovaleric acid (D-APV) and 20 μM 6,7-dinitroquinoxaline-2/3-dione (DNQX) in the external solution, and action potentials were blocked by using 1 μM tetrodotoxin (TTX) in the external solution. Bath application of the $GABA_A$ receptor antagonist bicuculline (5 μM) eliminated all currents observed, verifying that recorded currents were GABAergic mIPSCs.

Patch electrodes were filled with internal recording solution containing (in mM): CsCl 153.3, $MgCl_2$ 1.0, EGTA 5.0, and HEPES 10.0, with a pH of 7.40 and osmolarity of 290–300 mOsm. CsCl was used to block potassium currents. MgATP (4 mM) was included in the intracellular solution before recording. The external recording medium contained (in mM): NaCl 146.0, KCl 2.5, $MgCl_2$ 3.0, $CaCl_2$ 2.0, glucose 10.0, and HEPES 10.0, with a pH of 7.4 and

osmolarity of 315–330 mOsm. Internal and external solutions contained equimolar concentrations of chloride ions, and no $GABA_A$ receptor-mediated inhibitory postsynaptic currents (IPSCs) were evident at a clamped membrane potential of 0 mV. Recordings were made at a holding potential of −60 mV.

Neurons were studied on the stage of an inverted microscope at room temperature. Thick-walled (1.5 mm outer diameter, 0.86 mm inner diameter) borosilicate patch electrodes (World Precision Instruments, Sarasota, FL) were pulled on a P-97 Flaming-Brown horizontal puller (Sutter Instruments, Novarto, CA) by using a two-stage pull to a final resistance of 2–5 MΩ. Currents were recorded with an Axopatch 200A amplifier and low-pass filtered at 3 kHz with an eight-pole Bessel filter prior to digitization, storage, and display with the patch clamp technique (Hamill et al., 1981). Currents were recorded using Axoscope software (Axon Instruments, Burlingame, CA) digitized at 400 Hz. Series resistance and capacitance were compensated for each neuron. After baseline and input resistance became stable, mIPSC recordings were made for 5-minute epochs during 30–60 minutes.

Electrophysiological analysis

Pyramidal neurons were randomly selected for recording from two or more cultures. MiniAnalysis software (Synaptosoft, Decatur, GA) was used to analyze mIPSC frequency, amplitude, 10–90% rise time, and decay. Mean frequency is reported for 7 and 14 DIV. Frequency at 7 and 14 DIV was compared by using a Kolmogorov-Smirnov (K-S) test with a significance value of $P < 0.05$. Medians were measured for mIPSC amplitude and 10–90% rise time, because, in frequency histograms of each parameter, the frequency distributions were largely skewed to the right, so the mean of medians is reported for amplitude and 10–90% rise time at 7 and 14 DIV. Decay was analyzed by fitting with two-exponential curves and accepting the fit if $R^2 > 0.70$. Decays were analyzed until 20 values had been obtained for each neuron. Because the range of fitted mIPSC decays is also not normally distributed, the mean of median values of the decay of each neuron is also reported. For mIPSC amplitude, 10–90% rise time, and decay, values compared between two groups were analyzed by using a two-tailed Student's *t*-test with a significance value of $P < 0.05$. All values are reported ±SEM.

RESULTS

Emergence of nascent synapses

Comparisons of cultured hippocampal neurons prepared for immunocytochemistry at 3–7 DIV revealed that $GABA_A$ receptor clusters appeared before GABAergic terminals on pyramidal neurons. At 3 DIV, bright immunoreactive clusters of the γ2 (Fig. 1A) and β2/3 (Fig. 1D) $GABA_A$ receptors subunits were evident in all pyramidal cells, but immunoreactive puncta typical of presynaptic GAD-65 expression were not present (Fig. 1G). No mIPSCs could be recorded from any pyramidal neurons at 3 DIV (Fig. 1J), even when the cells were hyperpolarized to −80 mV to increase the Cl^- driving force (data not shown). However, at 7 DIV, γ2 subunit clusters (Fig. 1B), β2/3 subunit clusters (Fig. 1E), and GAD-65 puncta (Fig. 1H) were all visible, and mIPSCs could be recorded (Fig. 1K). The average size of GAD-65 puncta was greater than the average size of γ2 and β2/3 clusters (Table 1), because, unlike GAD-65, large clusters of γ2 and β2/3 are interspersed with very small clusters. The presence of postsynaptic markers together with presynaptic markers at 7 DIV but not 3 DIV suggested that nascent GABAergic synapses formed between 3 and 7 DIV. This process was studied in detail.

The appearance of synaptic activity lagged behind that of GABAergic markers. When the percentage of neurons containing GAD-65 puncta or mIPSCs was plotted as a function of DIV, mIPSCs lagged behind the appearance of GAD-65 cluster by half of a day (Fig. 1M). GAD-65 puncta and mIPSCs were first observed at 5 DIV. At this time, images captured with a ×20 objective (×20 fields, each containing 3–12 neurons) showed that 42.5% ± 4.2% of neurons contained GAD-65 puncta (n = 20 fields at ×20), but mIPSCs were observed in only 30% of neurons tested (n = 10 neurons). Both of these percentages increased until 7 DIV, when 92.9% ± 1.4% of neurons contained GAD-65 puncta (n = 20 fields at ×20), and mIPSCs were recorded from 83% of neurons analyzed (n = 6 neurons). By 8 DIV, GAD-65 puncta were present in all neurons examined (n = 20 fields at ×20), and mIPSCs were recorded from 94% of neurons tested (n = 17 neurons; at 4 DIV, n = 20 fields at ×20 for GAD-65 measurement and n = 9 neurons for mIPSC measurement; at 6 DIV, n = 17 fields at ×20 for GAD-65 analysis and n = 5 neurons for mIPSC recordings).

The size of γ2 and β2/3 subunit clusters increased during the appearance of GAD-65 puncta, which was interesting. The size of γ2 subunit clusters rose from 3 DIV (0.9 ± 0.05 μm diameter, n = 10 neurons) to 7 DIV (Table 1; $P < 0.05$), and the size of β2/3 subunit clusters increased from 3 DIV (1.1 ± 0.06 μm, n = 10 neurons) to 7 DIV (Table 1; $P < 0.001$).

Developmental increase in synapse number

GABAergic synapses proliferated during in vitro development. The number of presynaptic and postsynaptic markers per ×60 field increased from 7 to 14 DIV (Table 1; $P < 0.001$ for γ2 and $P < 0.0001$ for β2/3 and GAD-65) because of increased neuronal outgrowth during this time, as previously reported (Swanwick et al., 2004). Presynap-

Fig. 1. Emergence and proliferation of GABAergic synapses. Clusters of $GABA_A$ receptors were present before emergence of GABAergic presynaptic terminals, and the number of functional GABAergic synapses increased from 7 to 14 DIV. By 3 DIV, γ2 (**A**) and β2/3 (**D**) clusters had appeared, but GAD-65 puncta were not present (**G**). Arrows mark examples of clusters. However, at 7 DIV, clusters of γ2 (**B**), β2/3 (**E**), and GAD-65 (**H**) were all present, and they were increased in number at 14 DIV (**C,F,I**). Correspondingly, no mIPSCs were observed at 3 DIV (**J**), but some mIPSCs were recorded at 7 DIV (**K**), and mIPSC frequency was increased at 14 DIV (**L**). One-minute traces from three separate neurons are shown at 3 and 7 DIV, and 1-minute traces from two separate neurons are shown at 14 DIV. The percentages of neurons containing GAD-65 puncta or mIPSCs from 3 to 8 DIV were each best fit with a sigmoidal dose-response curve (**M**). These curves were tightly correlated, but the curve representing percentage of neurons with mIPSCs lagged approximately half of a day behind the curve illustrating percentage of neurons with GAD-65 puncta. Increased frequency of mIPSCs is shown with a cumulative frequency plot (**N**) for one neuron each at 7 and 14 DIV. The rates of colocalization of GAD-65 and γ2 (**O,P**) and GAD-65 and β2/3 (**Q,R**) also increased from 7 to 14 DIV. Images were captured at ×60. Scale bars = 10 μm.

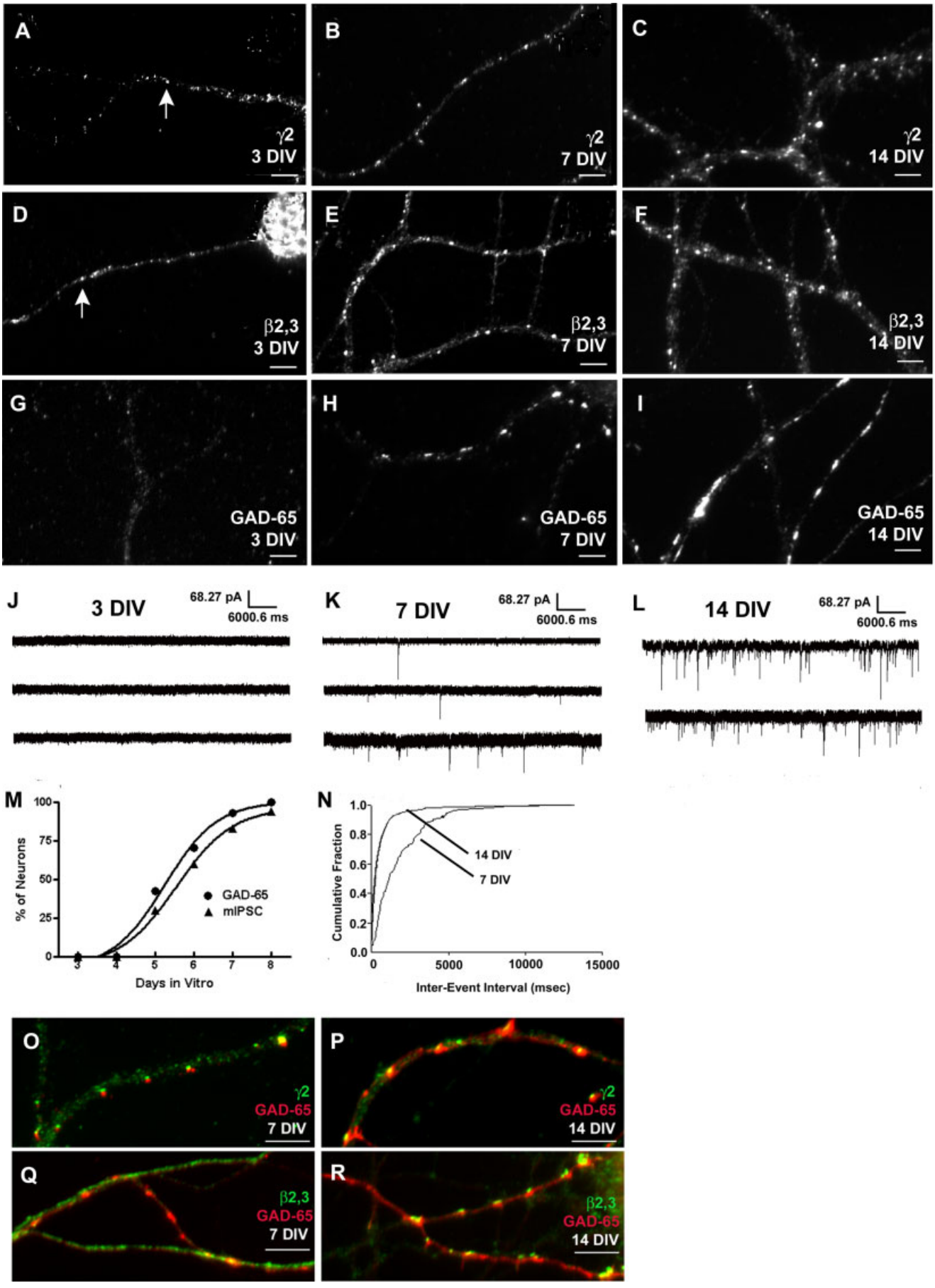
A
γ2
3 DIV
B
γ2
7 DIV
C
γ2
14 DIV
D
β2,3
3 DIV
E
β2,3
7 DIV
F
β2,3
14 DIV
G
GAD-65
3 DIV
H
GAD-65
7 DIV
I
GAD-65
14 DIV
J
3 DIV
68.27 pA
6000.6 ms
K
7 DIV
68.27 pA
6000.6 ms
L
14 DIV
68.27 pA
6000.6 ms
M
% of Neurons
Days in Vitro
GAD-65
mIPSC
N
Cumulative Fraction
Inter-Event Interval (msec)
14 DIV
7 DIV
O
γ2
GAD-65
7 DIV
P
γ2
GAD-65
14 DIV
Q
β2,3
GAD-65
7 DIV
R
β2,3
GAD-65
14 DIV

Figure 1

TABLE 1. Measurements of GABAergic Presynaptic and Postsynaptic Markers

	7 DIV	14 DIV
Number *(per neuron in × 60 field)*		
γ2 $P < 0.001$[1]	106.5 ± 8.2 (n = 33)	164.6 ± 13.6 (n = 37)
β2/3 $P < 0.0001$	109.0 ± 6.1 (n = 55)	181.3 ± 13.4 (n = 43)
GAD-65 $P < 0.0001$	76.2 ± 6.6 (n = 37)	151.9 ± 11.2 (n = 32)
Density *(per 10 μm²)*		
γ2	2.6 ± 0.5 (n = 16)	2.8 ± 0.3 (n = 16)
β2/3	2.5 ± 0.3 (n = 25)	3.2 ± 0.3 (n = 30)
GAD-65 $P < 0.0001$	1.2 ± 0.1 (n = 25)	2.5 ± 0.2 (n = 30)
α2	3.1 ± 0.5 (n = 12)	3.3 ± 0.5 (n = 12)
α5	N/A	2.8 ± 0.3 (n = 12)
GAT-1	N/A	2.3 ± 0.3 (n = 21)
GAT-3	4.4 ± 0.6 (n = 12)	4.2 ± 0.3 (n = 11)
Size (*μm diameter*)		
γ2 $P < 0.05$	1.3 ± 0.06 (n = 43)	1.6 ± 0.09 (n = 35)
β2/3	1.8 ± 0.07 (n = 51)	1.8 ± 0.07 (n = 57)
GAD-65 $P < 0.0001$	3.3 ± 0.3 (n = 51)	7.6 ± 0.5 (n = 44)
α2	2.2 ± 0.2 (n = 23)	2.1 ± 0.1 (n = 19)
α5	N/A	1.5 ± 0.2 (n = 12)
GAT-1	N/A	1.7 ± 0.4 (n = 21)
GAT-3	0.9 ± 0.1 (n = 12)	1.0 ± 0.1 (n = 11)
Synaptic localization (%)		
γ2 $P < 0.01$	37.2 ± 3.0 (n = 10)	57.1 ± 5.4 (n = 11)
β2/3 $P < 0.05$	31.7 ± 4.0 (n = 10)	46.4 ± 4.8 (n = 10)
α5	N/A	17.0 ± 2.3 (n = 12)
GAT-1	N/A	49.3 ± 7.2 (n = 11)
GAT-3	13.8 ± 3.0 (n = 12)	13.8 ± 2.3 (n = 10)

[1]*P* values are based on ANOVA and post hoc Bonferroni's multiple comparison test when β2/3 and γ2 subunit size were compared among DIV 3, 7, and 14 and unpaired *t*-test for other parameters, which were compared only between DIV 7 and DIV 14. n = Neurons.

TABLE 2. Measurements of mIPSC kinetics.

	7 DIV	14 DIV
Frequency (Hz) $P < 0.001$[1]	0.8 ± 0.2 (n = 11)	2.4 ± 0.7 (n = 17)
Amplitude (pA) $P < 0.01$	86.9 ± 11.0 (n = 11)	56.1 ± 3.9 (n = 17)
10–90% Rise time (msec) $P < 0.01$	1.3 ± 0.1 (n = 11)	1.8 ± 0.1 (n = 17)
τ_1 (msec) $P < 0.05$	30.5 ± 3.1 (n = 5)	23.5 ± 1.5 (n = 8)
τ_2 (msec)	98.5 ± 9.4 (n = 5)	81.6 ± 11.2 (n = 8)

[1]*P* values according unpaired *t*-test. n = Neurons.

tically, the density of GAD-65 puncta also rose from 7 DIV (Fig. 1H) to 14 DIV (Fig. 1I, Table 1; $P < 0.0001$). On the postsynaptic membrane, there was only a slight increase in the density of γ2 clusters (Fig. 1B,C) and β2/3 clusters (Fig. 1E,F) from 7 to 14 DIV (Table 1). However, the synaptic localization of γ2 and β2/3 subunit clusters rose from 7 to 14 DIV, as demonstrated by the percentage of γ2 and β2/3 subunit clusters colocalized with GAD-65 puncta approximately doubling from 7 DIV (Fig. 1O,Q) to 14 DIV (Fig. 1P,R, Table 1; $P < 0.01$ for γ2 and $P < 0.05$ for β2/3). The size of β2/3 clusters did not increase significantly from 7 to 14 DIV as they did from 3 to 7 DIV, in contrast to the size of γ2 clusters from 7 to 14 DIV (Table 1; $P < 0.05$). However, the size of GAD-65 puncta approximately doubled from 7 to 14 DIV (Table 1; $P < 0.0001$).

The new GABAergic synapses formed were functional. One-minute traces from 7 DIV neurons showed few mIPSCs present (Fig. 1K), whereas those from 14 DIV neurons showed numerous mIPSCs (Fig. 1L). A cumulative probability plot demonstrated that a higher fraction of mIPSCs recorded from 14 DIV neurons had shorter interevent intervals than mIPSCs recorded from 7 DIV neurons (Fig. 1N). Mean mIPSC frequency increased threefold from 7 to 14 DIV (Table 2; $P < 0.001$).

New synapses were located on distal dendrites

The increased number of GABAergic synapses per neuron might have resulted from either of two possibilities: 1) increased density of GABAergic synapses or 2) constant density of GABAergic synapses but increased area resulting from outgrowth of neuronal processes. The density of γ2 and β2/3 receptor clusters remained constant, but the number of neuronal processes increased from 7 to 14 DIV, as mentioned above, suggesting that the latter explanation holds for the increased density of GABAergic synapses per neuron. Moreover, whole-cell capacitance increased from 7.2 ± 0.9 pF at 7 DIV (n = 11 neurons) to 10.1 ± 1.3 pF at 14 DIV (n = 16 neurons), confirming that these neurons grow and their processes elongate during in vitro development.

In support of this, the mean distance of presynaptic GAD-65 puncta from the soma increased during in vitro development as a result of increased neuronal outgrowth. Images captured with a ×20 objective show GAD-65 puncta distributed throughout neuronal processes at both 7 DIV (Fig. 2A) and 14 DIV (Fig. 2B) but an increased number and length of processes at 14 DIV. The distances of GAD-65 puncta from the soma at both days were calculated by drawing concentric regions around the soma in 25-μm-diameter increments, so that puncta were classified into the following distances from the soma: 0–25 μm, 26–50 μm, 51–75 μm, 76–100 μm, 101–125 μm, 126–150 μm, 151–175 μm, and 176–200 μm. At 7 DIV, most dendrites were located within 150 μm of the soma. At 14 DIV, the dendritic arbor was more complex, and several dendrites extended beyond the edges of the last concentric circle, which had a boundary of 200 μm from the soma. The number of synapses in each distance category was quantified. Whereas at 7 DIV the somatic distances were concentrated around smaller values and highest at 0–25 μm and 25–50 μm (n = 5 neurons; Fig. 2C), at 14 DIV the distribution of somatic distances shifted rightward toward higher values and the greatest distances moved to 75–100 μm (n = 5 neurons; Fig. 2D). This shift is similar to that reported from a Scholl analysis by Benson and Cohen (1996). However, these calculations of physical distance actually underestimate the electrical distance of synapses from the soma, insofar as outgrowth of neuronal processes does not always proceed linearly from the soma; some neurites may also curve back toward the soma as they grow and might therefore have been included in a category of smaller distance.

Synaptic currents generated by newly formed distal synapses are expected to be slowed and attenuated by increased electrical distance. In support of this, the 10–90% rise time of mIPSC recorded from neurons slowed from 7 to 14 DIV (Table 2; $P < 0.01$). A frequency distribution histogram of mIPSC rise times showed a peak centered slightly above 1 msec at 7 DIV (Fig. 2H), whereas, at 14 DIV (Fig. 2I), the distribution was skewed, with a large number of 10–90% rise times ranging from 2 to 3 msec. In addition, mIPSC amplitude decreased from 7 to 14 DIV (Table 2; $P < 0.01$). Average mIPSC traces recorded from pyramidal neurons at 14 DIV were much smaller than at 7 DIV (Fig. 2E). A frequency distribution histogram of mIPSC amplitudes recorded from a neuron at 7 DIV displays a wide distribution and many large values, including many amplitudes ranging from 200 to 400 pA (Fig. 2F), whereas, in the histogram from a neuron at 14 DIV, the number of amplitudes ranging from 0 to 200 pA was disproportionately higher (Fig. 2G). Therefore, despite maximal compensation for resistance and capaci-

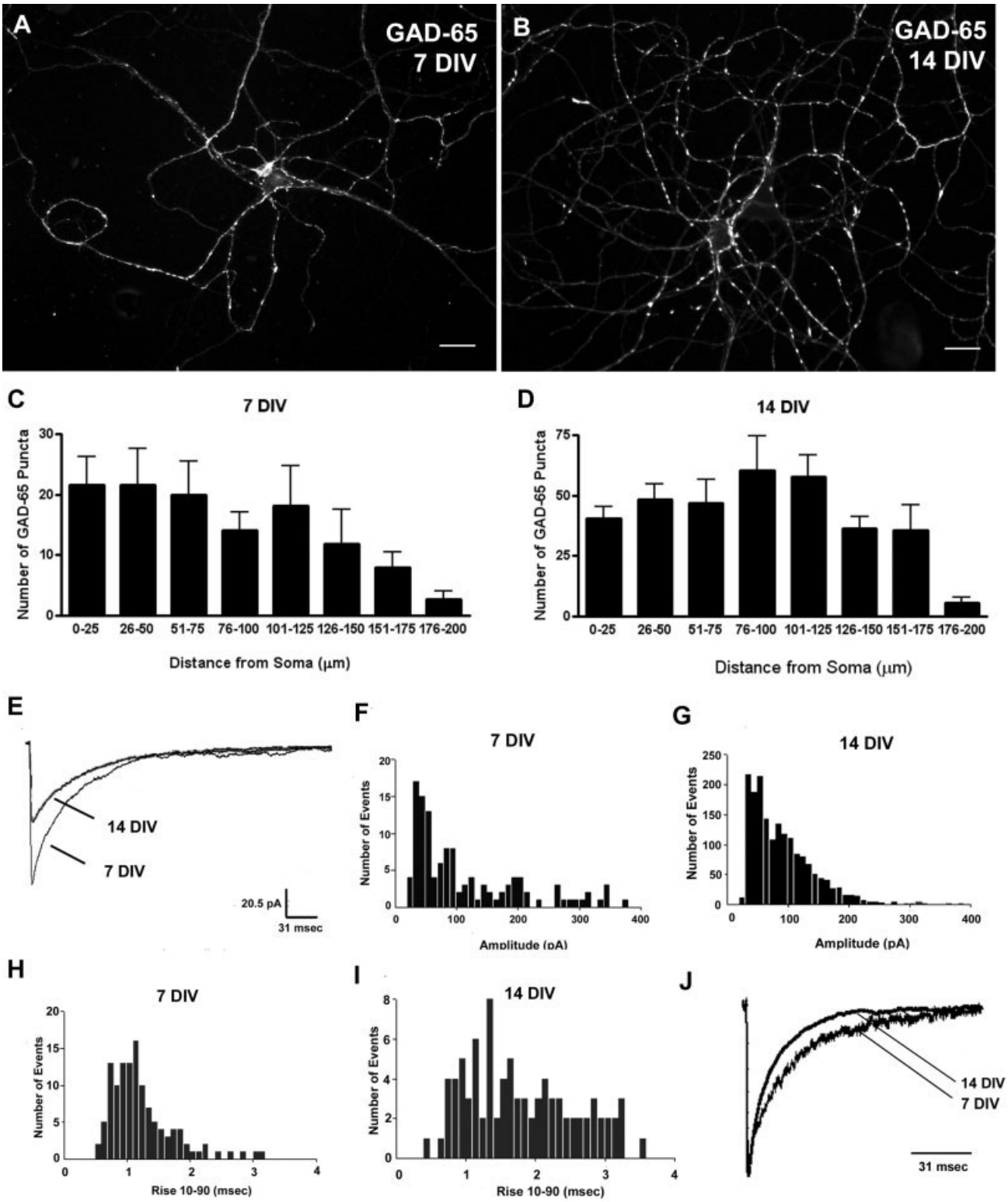

Fig. 2. Distal formation of GABAergic synapses from 7 to 14 DIV. Distance of GAD-65 puncta from the soma increased from 7 DIV (**A,C**) to 14 DIV (**B,D**) because of increased outgrowth of neuronal processes. Amplitude of mIPSCs decreased from 7 to 14 DIV (**E–G**). Average mIPSC trace at 7 DIV is larger than at 14 DIV (E). A frequency histogram of mIPSC amplitudes at 7 DIV (F) shifts leftward at 14 DIV (G); 10–90% rise time of mIPSCs slowed from 7 to 14 DIV (**H,I**). A frequency histogram of mIPSC 10–90% rise time at 7 DIV (H) shifts rightward at 14 DIV (I). mIPSC decay also quickened from 7 to 14 DIV, as shown by average mIPSC traces normalized for amplitude (J). Images were captured at ×20. Scale bars = 20 μm.

tance in pyramidal neurons, distal mIPSCs were filtered as they traveled to the somatic site of recording.

Another possible explanation for decreased mIPSC amplitude is a reduced number of synaptic $GABA_A$ receptors. However, as mentioned above, the size of γ2 and β2/3 subunit clusters, which should approximately correspond to the number of receptors present, did not diminish from 7 to 14 DIV (Table 1). Alternatively, mIPSC amplitude could have declined because of a decrease in single channel conductance (Sigworth, 1981; Johnston and Wu, 1995; Cohen et al., 2000). However, when single channel conductance was estimated bu using nonstationary analysis, it had not significantly changed from 7 to 14 DIV.

Expression of $GABA_A$ receptor subunits

In addition to increased frequency, diminished amplitude, and slowed 10–90% rise time, the decay of mIPSCs quickened from 7 to 14 DIV. Decays of mIPSCs were best fit with a biexponential curve, where τ_1 represented the fast component of decay and τ_2 represented the slow component of decay. mIPSCs at 7 DIV returned to baseline current slower than mIPSCs at 14 DIV (Fig. 2H). Average mIPSC traces at 14 DIV were smoother than at 7 DIV, because frequency increased during development. When mIPSC decay was quantified, τ_1 shortened from 7 to 14 DIV (Table 2; $P < 0.05$), whereas τ_2 remained relatively constant from 7 to 14 DIV (Table 2).

The mIPSC kinetics may be shaped by $GABA_A$ receptor subunit composition (McKernan and Whiting, 1996). Therefore, the distributions of the α1, α2, α4, α5, and δ subunits of the $GABA_A$ receptor were examined at 7 and 14 DIV (Fig. 3). The α2 subunit immunoreactivity was clustered at 7 DIV (Fig. 3A) and 14 DIV (Fig. 3B), and the density and size of these clusters remained relatively constant during this time (Table 1).

The α4 subunit immunoreactivity was diffusely distributed at 7 and14 DIV (Fig. 3C,D). The δ subunit, which is commonly coassembled with the α4 subunit (McKernan and Whiting, 1996), was also expressed diffusely from 7 to 14 DIV, although it showed some tiny puncta no larger than nonspecific labeling (Fig. 3E,F). The absence of α4 and δ clusters on pyramidal neurons suggests that these subunits were not synaptic at either time point.

However, distribution of the α5 subunit immunoreactivity changed from 7 to 14 DIV. At 7 DIV, cell bodies of pyramidal neurons were diffusely stained for α5, with nonspecific granular labeling spread throughout the processes (Fig. 3G). However, at 14 DIV, the cell body was still intensely labeled, but large clusters of α5 immunoreactivity had emerged in the neuronal processes (Fig. 3H). These α5 immunoreactive clusters were relatively dense and fairly small (Table 1). Only a small fraction of α5 clusters at 14 DIV was apposed to GABAergic presynaptic terminals (Fig. 3I, Table 1). Clusters of α5 were no longer present at 21 DIV (data not shown).

Clusters of α1 subunit immunoreactivity fully emerged in pyramidal neurons only by 21 DIV (Fig. 4). In pyramidal neurons at 7 DIV, α1 subunit staining (Fig. 4A) was diffuse, although large, distinct α1 subunit clusters were found on interneurons in the same cultures (data not shown). At 14 DIV (Fig. 4B), although approximately 20% of pyramidal neurons contained larger α1 subunit clusters similar to ones found on interneurons, the majority of pyramidal neurons displayed a mostly diffuse pattern of staining for this subunit. However, at 21 DIV, approximately 80% of pyramidal neurons contained abundant large, intense clusters of α1 immunoreactivity scattered throughout the neuronal processes (Fig. 4C). The density

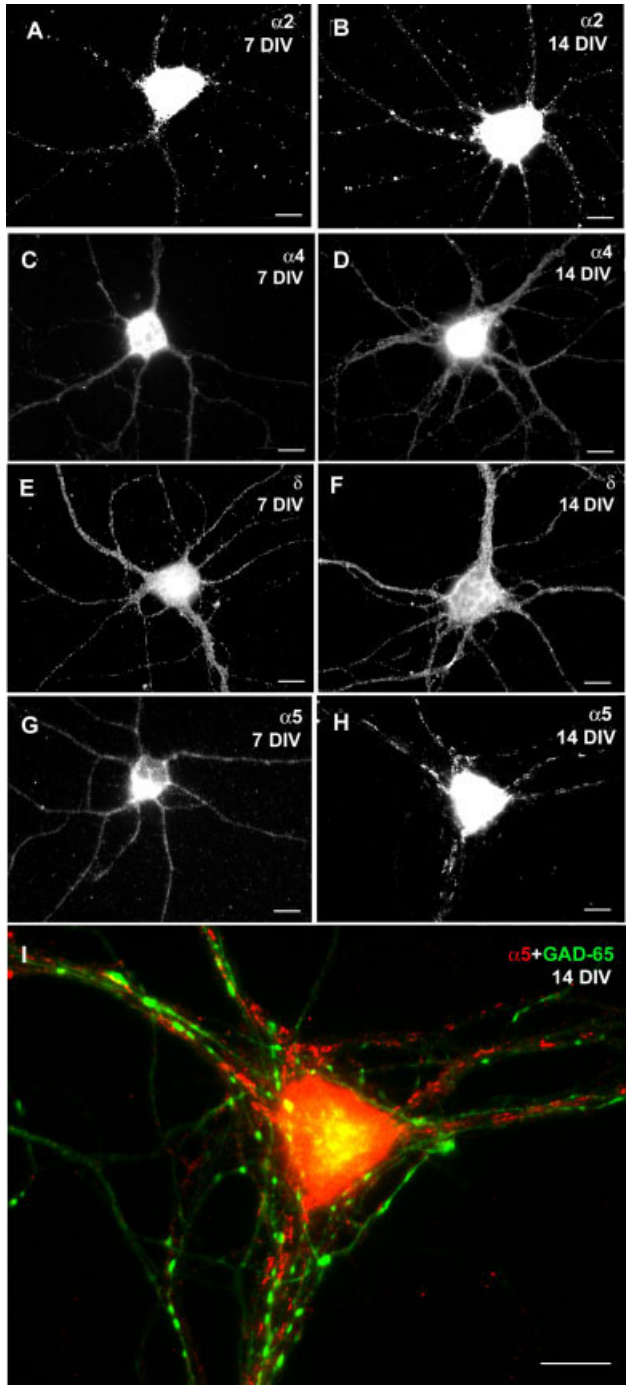

Fig. 3. Alterations in $GABA_A$ receptor subunit composition from 7 to 14 DIV. The α2 subunit remained clustered increased from 7 to 14 DIV (**A,B**). The α4 (**C,D**) and δ (**E,F**) subunits were mostly diffusely distributed from 7 to 14 DIV. The α5 subunit was mostly diffusely distributed at 7 DIV (**G**) but became clustered at 14 DIV (**H**). Most α5 clusters at 14 DIV were not colocalized with GAD-65 puncta (**I**). Images were captured at ×60. Scale bars = 10 μm.

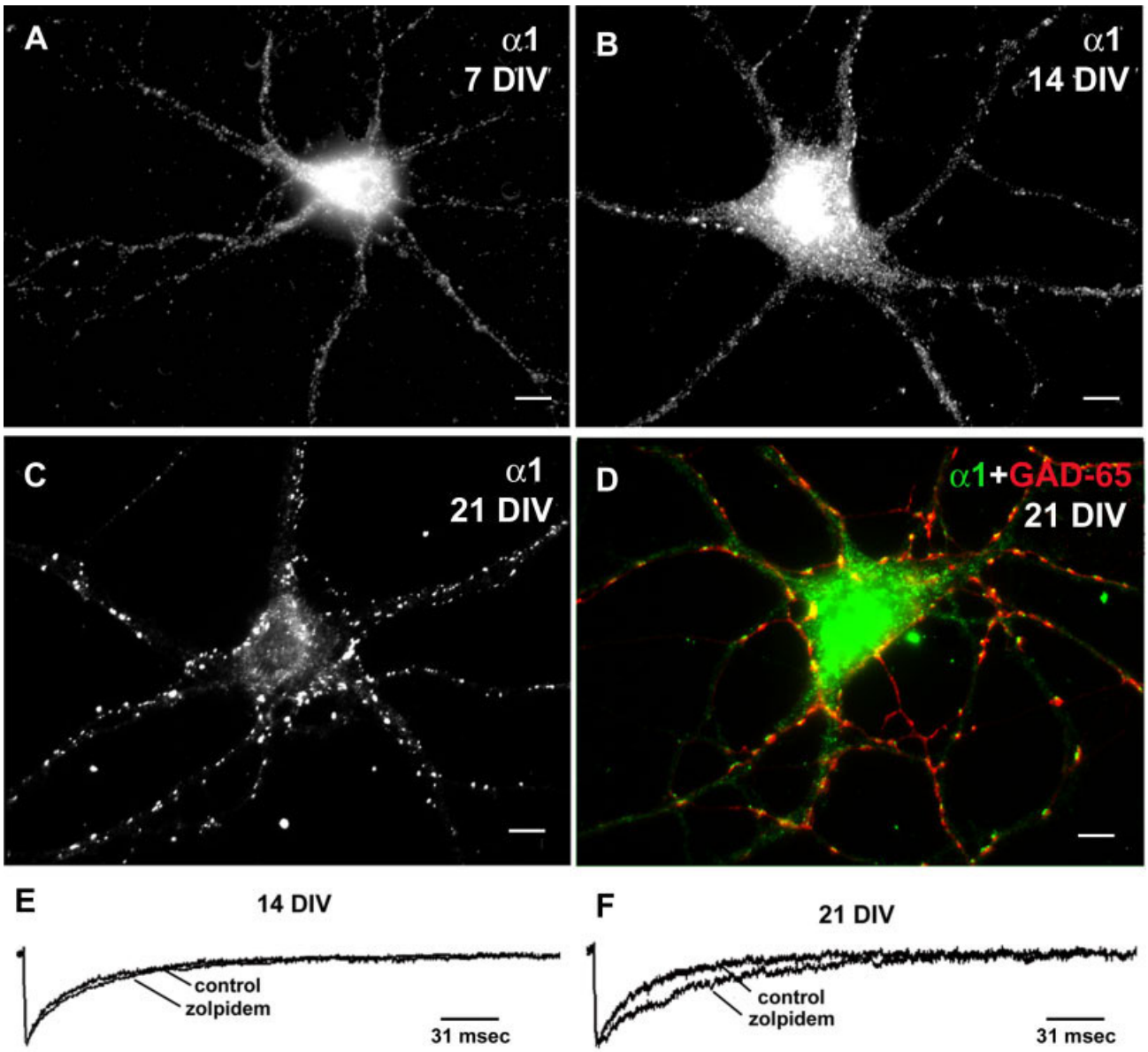

Fig. 4. Expression of the α1 subunit of the $GABA_A$ receptor from 7 to 21 DIV. Distribution of α1 subunits was mostly diffuse at 7 DIV (**A**). Approximately 20% of pyramidal neurons contained some small α1 clusters at 14 DIV (**B**), but α1 clusters fully emerged by 21 DIV (**C**). Most α1 clusters at 21 DIV were colocalized with GAD-65 puncta (**D**). In confirmation, treatment with 30 nM zolpidem, an α1 subunit selective agonist, had no effect on mIPSCs at 14 DIV (**E**) but prolonged decay at 21 DIV (**F**). Average mIPSC traces shown were normalized for amplitude. Images were captured at ×60. Scale bars = 10 μm.

of α1 clusters per 10 μm^2 at this time was 2.7 ± 0.4 (n = 13 neurons), and the diameter of the clusters was 3.4 ± 0.2 μm (n = 33 neurons). Many α1 clusters (55.5% ± 5%, n = 11 neurons; Fig. 4D) overlapped with GAD-65 puncta, indicating that they were apposed to GABAergic presynaptic terminals.

To confirm this immunocytochemical data regarding α1 expression, mIPSCs were recorded in pyramidal neurons at 14 and 21 DIV before and after bath application of zolpidem (30 nM), a drug that potentiates $GABA_A$ receptors containing the α1 subunit. Average mIPSC traces from a neuron at 21 DIV in the presence of zolpidem had more prolonged decay than those before drug application (Fig. 4F). The second component of mIPSC decay, τ_2 was significantly prolonged from 101.4 ± 12.2 msec before treatment (n = 5 neurons) to 148.8 ± 22.6 msec after zolpidem (n = 5 neurons, $P < 0.05$), but τ_1 remained unchanged, going from 24.0 ± 1.8 msec to 23.2 ± 1.8 msec. In contrast, at 14 DIV, average mIPSC traces from the same pyramidal neuron before and after zolpidem treatment looked similar (Fig. 4E), and neither component of the decay was significantly affected, (τ_1: 24.4 ± 1.7 msec vs. 23.8 ± 1.2 msec, n = 5 neurons; τ_2: 91.8 ± 8.1 msec vs. 93.9 ± 10.0 msec, n = 5 neurons).

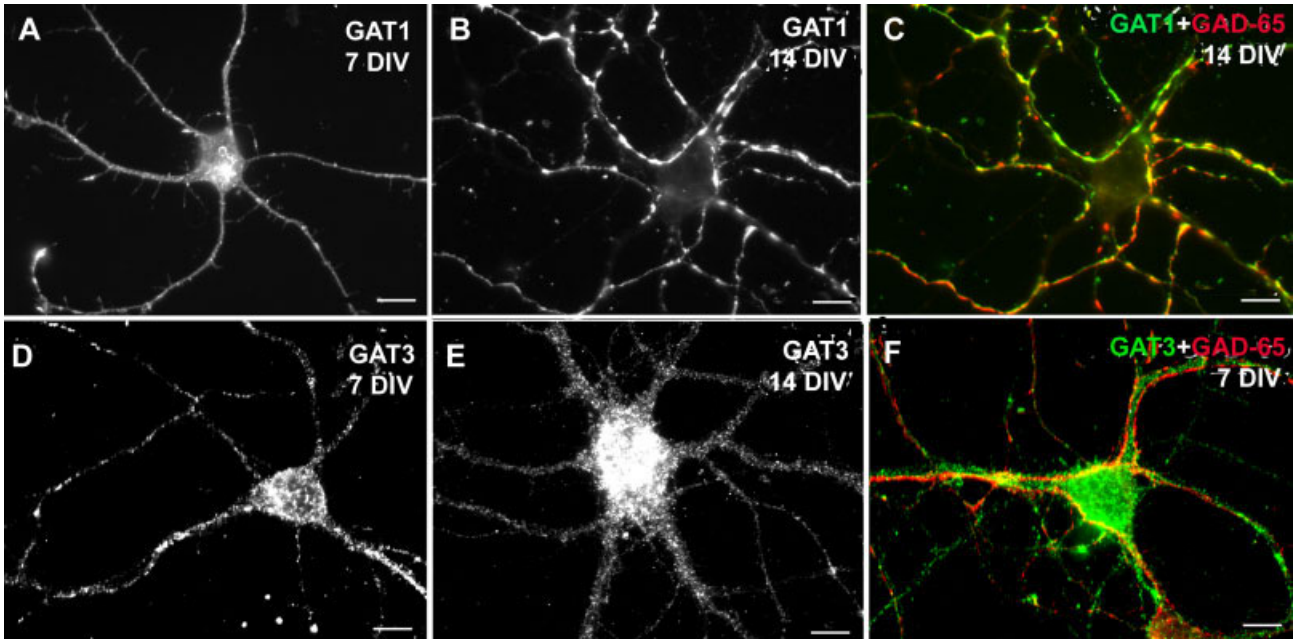

Fig. 5. Expression of GAT-1 and GAT-3 from 7 to 14 DIV. GAT-1 puncta emerged by 14 DIV (**A,B**). Most GAT-1 puncta at 14 DIV were colocalized with GAD-65 puncta (**C**). Small GAT-3 puncta were constantly present from 7 to 14 DIV (**D,E**). Most of these small GAT-3 puncta were not colocalized with GAD-65 puncta (**F**). Images were captured at ×60. Scale bars = 10 μm.

GABA transporter expression

There are four identified GABA transporters (GATs; Guastella et al., 1990; Borden et al., 1992; Liu et al., 1993). GAT-2 and GAT-4 (also known as "BGT-1") are expressed in both the peripheral and the central nervous systems, but in the brain GAT-2 is limited to the meninges (Ikegaki et al., 1994), and GAT-4 is most concentrated in the anterior hypothalamus and septal area (Borden, 1996). However, the expression of GABA transporters GAT-1 and GAT-3 is developmentally regulated in the hippocampus and cortex (Vitellaro-Zuccarello et al., 2003; Sipilä et al., 2004), so the expression of these GABA transporter subtypes was examined during in vitro development.

GAT-1 distribution was altered from 7 to 14 DIV. At 7 DIV, GAT-1 immunoreactivity was mostly diffuse (Fig. 5A), with small puncta present in some neurons. However, at 14 DIV, GAT-1 expression appeared strong and punctate (Fig. 5B, Table 1). Many GAT-1 puncta overlapped with GAD-65 puncta at 14 DIV, suggesting that these GAT-1 puncta at 14 DIV were synaptic (Table 1).

In contrast, small GAT-3 puncta were constantly present from 7 to 14 DIV. GAT-3 was densely distributed as small, granular puncta at both 7 DIV (Fig. 5D) and 14 DIV (Fig. 5E, Table 1). Few GAT-3 puncta overlapped with GAD-65 puncta (Fig. 5F, Table 1), implying that most GAT-3 puncta were extrasynaptic.

DISCUSSION

This study provides to the best of our knowledge the first description of the relationship between functional maturation of GABAergic synapses with the development of various pre- and postsynaptic elements. The primary conclusions are that during in vitro development of GABAergic synapses 1) the onset of mIPSCs lags behind the formation of receptor clusters and GAD-65 puncta; 2) functional GABAergic synapses increase in number distally because of neuronal outgrowth, resulting in more frequent mIPSCs with slower rise times and smaller amplitudes; 3) decay of mIPSCs quickens; and 4) clusters of the α5 subunit of the $GABA_A$ receptor and puncta of GAT-1 emerge. A summary of molecular and functional alterations during GABAergic synaptogenesis is given in Figure 6.

Emergence of GABAergic synapses

Clusters of $GABA_A$ receptors were present early and increased in number during in vitro development. Other authors also report that $GABA_A$ receptor clusters are present in the dendrites, soma, and axon initial segment of pyramidal neruons as early as 3–4 DIV (Christie et al., 2002; Christie and De Blas, 2003; Elmariah et al., 2004, 2005), and some even describe the emergence of GABA receptor clusters 6 hours after plating (Scotti and Reuter, 2001). The emergence of presynaptic GABAergic terminals lagged behind that of $GABA_A$ receptor clusters, but terminals also grew in number during in vitro development. Another marker of presynaptic GABAergic terminals, vesicular inhibitory amino acid transporter, rarely appeared as puncta at 4 DIV but was expressed as numerous puncta at 7 and 10 DIV (Elmariah et al., 2005). In the absence of GABAergic innervation, the $GABA_A$ receptor clusters are mismatched with presynaptic glutamatergic terminals, but, upon GABAergic innervation, the $GABA_A$ receptor clusters become aligned with presynaptic GABAergic terminals (Rao et al., 2000; Christie et al.,

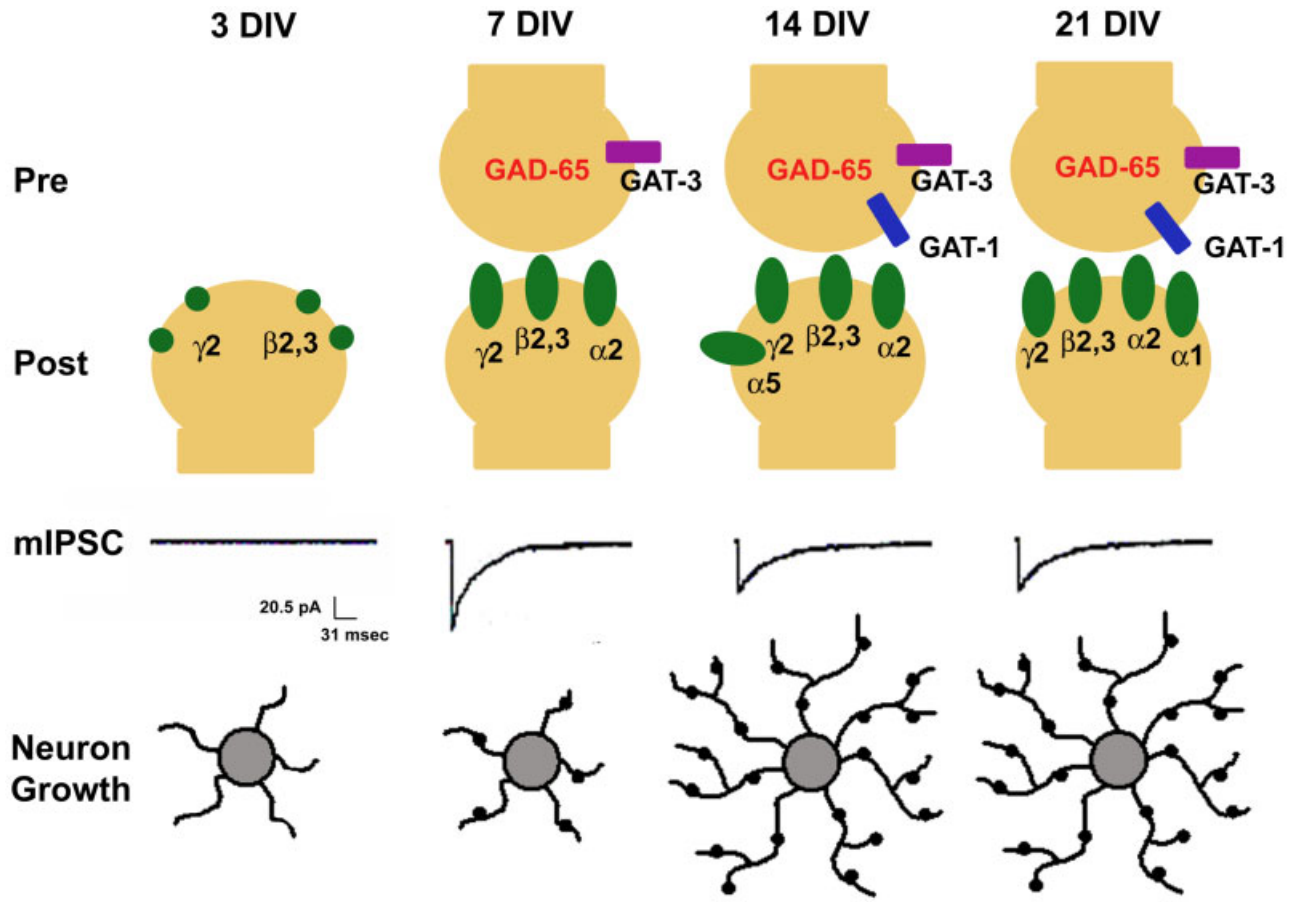

Fig. 6. Summary of GABAergic synaptogenesis in cultured hippocampal neurons. Postsynaptic specializations were present by 3 DIV, but presynaptic terminals emerged only at 5 DIV. mIPSC onset coincided with first appearance of presynaptic terminals. Most neurons displayed mIPSCs by 7 DIV. Synapses increased in number distally from the soma from 7 to 14 DIV, mostly because of elongation of neuronal processes, causing decreased mIPSC amplitude and slowed mIPSC 10–90% rise time between these time points. Whereas the α4 and δ subunits of the $GABA_A$ receptor remained diffuse at 7 and 14 DIV, the γ2 and β2/3 subunits became clustered by 3 DIV, the α2 subunit was clustered at 7 and 14 DIV, the α5 subunit became clustered by 14 DIV but was not clustered at 21 DIV, and the α1 subunit became clustered by 21 DIV. GAT-1 puncta emerged by 14 DIV, whereas GAT-3 appeared at 7 and 14 DIV. Most γ2, β2/3, α2, α1, and GAT-1 clusters were synaptic, whereas most α5 and GAT-3 clusters were extrasynaptic. Black circles indicate GABAergic synapses.

2002; Christie and De Blas, 2003). Measurements of synaptic localization equivalent to the present study were obtained in a similar neuron–glia coculture system, in which approximately one-third of $GABA_A$ receptor clusters were synaptically localized by the end of the first week in vitro and two-thirds were synaptically localized by the end of the second week in vitro (Elmariah et al., 2004, 2005).

Preexisting $GABA_A$ receptor clusters became larger during the emergence of presynaptic terminals, as in previous studies (Christie et al., 2002; Christie and De Blas, 2003). The increased cluster size corresponded to increased synaptic localization, suggesting that extrasynaptic $GABA_A$ receptors are being recruited into synapses. Indeed, when $GABA_A$ receptor clusters became larger, surrounding smaller $GABA_A$ receptor clusters disappeared, which is similar to observations made by Christie et al. (2002). The formation of larger clusters may be mediated either by the assembly of newly synthesized $GABA_A$ receptor clusters or by the aggregation of smaller clusters. This aggregation could occur through lateral membrane diffusion or through internalization and reinsertion in the cell membrane. Signals that might mediate either of these processes are unknown.

An important question is whether clusters of $GABA_A$ receptors alone possess functional capability. Whereas neurons containing clusters of $GABA_A$ receptors alone did not exhibit mIPSCs, the present study did not analyze the onset of action potential-dependent spontaneous IPSCS (sIPSCs). Recent studies demonstrated paracrine release of GABA before synapse formation (Demarque et al., 2002) and that 50% of cortical neurons contained sIPSCs at birth (Owens et al., 1999). It is possible that mIPSCs and sIPSCs depend on different cellular release mechanisms. In support of this, Sara and colleagues (2005) recently showed that activity-dependent and activity-independent currents involve the release of vesicles from different pools. This suggests that the hippocampal neurons used in the present study may possess release machinery necessary for sIPSCs but lacked the appropriate signals to induce mIPSCs before they were joined together with nascent presynaptic terminals.

Maturation of GABAergic synapses

There were striking molecular and functional differences between nascent GABAergic synapses and GABAergic synapses in relatively mature pyramidal neurons. The mIPSC rise time, amplitude, and decay recorded from immature neurons were vastly different from those in more developed neurons. Similar alterations in mIPSC kinetics have also been reported in CA1 pyramidal neurons during postnatal development (Cohen et al., 2000). Only α2, β2/3, and γ2 subunit-containing receptor clusters were present in nascent synapses, whereas α1, α5, α2, β2,3, and γ2 subunit-containing receptors were expressed at GABAergic synapses in developing pyramidal neurons.

Clusters of α5 subunit-containing $GABA_A$ receptors were present only in relatively mature pyramidal neurons. The presence of α5 subunits at GABAergic synapses might have contributed to altered mIPSC decay, insofar as the α5 subunit is thought to be critical in determining the dominant kinetics of $GABA_A$ receptors (Serafini et al., 1998). Previous studies have also shown clusters of α5 in relatively mature neurons (Christie and De Blas, 2002; Brunig et al., 2002), and the larger clusters may be synaptic (Christie and De Blas, 2002). Overall α5 subunit mRNA and protein levels generally decline during postnatal development (Laurie et al., 1992; Poulter et al., 1992; Hutcheon et al., 2004), implying that the reduced α5 subunit protein is redistributed into clusters. In confirmation, Ramos et al. (2004) showed a developmental change in α5 subunit distribution in hippocampal CA1 slices, in which α5 immunoreactivity was expressed in cell bodies early and descended into dendrites later during postnatal development. However, single-cell mRNA amplification revealed that α5 mRNA increased transiently in hippocampal neurons from approximately 7 to 14 DIV but then declined (Brooks-Kayal et al., 1998), introducing the alternative explanation that emergence of α5 clusters at 14 DIV correlates with this transient α5 mRNA increase. In support, at ~21 DIV, α5 clusters were either weakly stained (Brunig et al., 2002) or not present.

Previous studies have suggested that a developmental decrease in mIPSC decay may be due to a switch in expression from α2 subunit-containing $GABA_A$ receptors to α1 subunit-containing $GABA_A$ receptors (Lavoie et al., 1997; Okada et al., 2000; Juttner et al., 2001; Vicini et al., 2001; Bosman et al., 2002; Goldstein et al., 2002). This study revealed that the distributions of α2 and α1 subunit immunoreactivity were unaltered between 7 and 14 DIV, although the clustering of α1 subunit-containing $GABA_A$ receptors is just beginning at 14 DIV. This suggests that changes in expression of α2 and α1 subunits do not occur during this period, although quantitative methods such as Western blotting would be needed for verification. Moreover, synaptic α1 subunit clusters fully emerged only by 21 DIV, suggesting that α1 subunit clusters may influence mIPSC kinetics later during in vitro development. Previous studies on mature cultured hippocampal neurons have reported similarly that both α1 and α2 clusters are synaptic (Brunig et al., 2002; Christie et al., 2002; Mangan et al., 2005).

Another possible explanation for prolonged mIPSC decay at 7 DIV is the presence of α4 and δ subunits exclusively at this time. The α4 subunit preferentially combines with the δ subunit (McKernan and Whiting, 1996), and the δ subunit prolongs desensitization of whole-cell currents (Saxena and Macdonald, 1994) and preferentially desensitizes with slow and ultraslow phases of desensitization of recombinant receptors (Bianchi and Macdonald, 2002). However, the expression of α4 and δ subunits was not clustered at 7 DIV; immunostaining for these subunits was diffusely distributed at both 7 and 14 DIV.

It should be noted that developmental alterations in the nature of GABAergic synaptic transmission have been well established. In the neonatal brain, GABA depolarizes and excites neuronal membranes (Ben-Ari, 2002). However, starting from the end of the first postnatal week of life, GABA becomes inhibitory by a delayed expression of a Cl^- exporter, leading to a negative shift in the reversal potential for chloride ions (Rivera et al., 1999; Ben-Ari, 2002). However, the present study recorded mIPSCs using equimolar concentrations of chloride ions in the pipette and external solutions, so this change in Cl^- reversal potential could not have been responsible for the alterations in mIPSC kinetics that were observed.

Maturation of GABA transporters

Whereas GAT-3 was constantly expressed as small puncta during in vitro development, GAT-1 was present only in more mature pyramidal neurons. Furthermore, because many GAT-1 puncta were synaptic, unlike GAT-3 puncta, it is tempting to speculate that this localization may cause increased reuptake of synaptic GABA, thereby affecting the mIPSC kinetics observed in this study. However, the contribution of GABA transporters to mIPSC kinetics is thought to be limited. Whereas GABA transporter blockers prolonged evoked IPSCs (Dingledine and Korn, 1985; Roepstorff and Lambert, 1992, 1994; Thompson and Gahwiler, 1992; Isaacson et al., 1993; Draguhn and Heinemann, 1996), this effect was not evident in smaller evoked currents, sIPSCs, or mIPSCs, suggesting that transporters promote GABA clearance only when large numbers of release sites are activated (Thompson and Gahwiler, 1992; Isaacson et al., 1993; Roepstorff and Lambert, 1994; Nusser and Mody, 2002; Jensen et al., 2003; Overstreet and Westbrook, 2003).

In summary, this study showed that, during GABAergic synaptogenesis in cultured hippocampal neurons, the expression of GABAergic synaptic proteins correlated with alterations in synaptic function. mIPSCs appeared after both presynaptic and postsynaptic elements were present and functional GABAergic synapses increased in number distally during in vitro development. In addition, kinetics of GABAergic synaptic currents were altered during maturation of GABAergic synapses, corresponding to their composition.

ACKNOWLEDGMENTS

We thank Ms. Cassie Gregory, Ms. Ashley Renick, and Ms. Bahar Alawi for preparing and maintaining the hippocampal cultures. We also thank Dr. Howard Goodkin for constructive comments on the article. The generation of antibodies was supported by the Austrian Science Fund.

LITERATURE CITED

Ahmari SE, Smith SJ. 2002. Knowing a nascent synapse when you see it. Neuron 34:333–336.

Ben Ari Y. 2002. Excitatory actions of GABA during development: the nature of the nurture. Nat Rev Neurosci 3:728–739.

Bencsits E, Ebert V, Tretter V, Sieghart W. 1999. A significant part of native gamma-aminobutyric Acid A receptors containing α4 subunits do not contain γ or δ subunits. J Biol Chem 274:19613–19616.

Benson DL, Cohen PA. 1996. Activity-independent segregation of excitatory and inhibitory synaptic terminals in cultured hippocampal neurons. J Neurosci 16:6424–6432.

Benson DL, Watkins FH, Steward O, Banker G. 1994. Characterization of GABAergic neurons in hippocampal cell cultures. J Neurocytol 23:279–295.

Bianchi MT, Macdonald RL. 2002. Slow phases of $GABA_A$ receptor desensitization: structural determinants and possible relevance for synaptic function. J Physiol 544:3–18.

Borden LA. 1996. GABA transporter heterogeneity: pharmacology and cellular localization. Neurochem Int 29:335–356.

Borden LA, Smith KE, Hartig PR, Branchek TA, Weinshank RL. 1992. Molecular heterogeneity of the gamma-aminobutyric acid (GABA) transport system. Cloning of two novel high affinity GABA transporters from rat brain. J Biol Chem 267:21098–21104.

Bosman LW, Rosahl TW, Brussaard AB. 2002. Neonatal development of the rat visual cortex: synaptic function of $GABA_A$ receptor alpha subunits. J Physiol 545:169–181.

Brandon NJ, Delmas P, Kittler JT, McDonald BJ, Sieghart W, Brown DA, Smart TG, Moss SJ. 2000. $GABA_A$ receptor phosphorylation and functional modulation in cortical neurons by a protein kinase C-dependent pathway. J Biol Chem 275:38856–38862.

Brooks-Kayal AR, Jin H, Price M, Dichter MA. 1998. Developmental expression of $GABA_A$ receptor subunit mRNAs in individual hippocampal neurons in vitro and in vivo. J Neurochem 70:1017–1028.

Brunig I, Scotti E, Sidler C, Fritschy JM. 2002. Intact sorting, targeting, and clustering of gamma-aminobutyric acid A receptor subtypes in hippocampal neurons in vitro. J Comp Neurol 443:43–55.

Chang YC, Gottlieb DI. 1988. Characterization of the proteins purified with monoclonal antibodies to glutamic acid decarboxylase. J Neurosci 8:2123–2130.

Christie SB, De Blas AL. 2002. α5 Subunit-containing GABA(A) receptors form clusters at GABAergic synapses in hippocampal cultures. Neuroreport 13:2355–2358.

Christie SB, De Blas AL. 2003. GABAergic and glutamatergic axons innervate the axon initial segment and organize $GABA_A$ receptor clusters of cultured hippocampal pyramidal cells. J Comp Neurol 456:361–374.

Christie SB, Miralles CP, De Blas AL. 2002. GABAergic innervation organizes synaptic and extrasynaptic $GABA_A$ receptor clustering in cultured hippocampal neurons. J Neurosci 22:684–697.

Cohen AS, Lin DD, Coulter DA. 2000. Protracted postnatal development of inhibitory synaptic transmission in rat hippocampal area CA1 neurons. J Neurophysiol 84:2465–2476.

Craig AM, Blackstone CD, Huganir RL, Banker G. 1994. Selective clustering of glutamate and gamma-aminobutyric acid receptors opposite terminals releasing the corresponding neurotransmitters. Proc Natl Acad Sci U S A 91:12373–12377.

Demarque M, Represa A, Becq H, Khalilov I, Ben Ari Y, Aniksztejn L. 2002. Paracrine intercellular communication by a Ca^{2+}- and SNARE-independent release of GABA and glutamate prior to synapse formation. Neuron 36:1051–1061.

Dingledine R, Korn SJ. 1985. Gamma-aminobutyric acid uptake and the termination of inhibitory synaptic potentials in the rat hippocampal slice. J Physiol 366:387–409.

Draguhn A, Heinemann U. 1996. Different mechanisms regulate IPSC kinetics in early postnatal and juvenile hippocampal granule cells. J Neurophysiol 76:3983–3993.

Dupuy ST, Houser CR. 1996. Prominent expression of two forms of glutamate decarboxylase in the embryonic and early postnatal rat hippocampal formation. J Neurosci 16:6919–6932.

Elmariah SB, Crumling MA, Parsons TD, Balice-Gordon RJ. 2004. Postsynaptic TrkB-mediated signaling modulates excitatory and inhibitory neurotransmitter receptor clustering at hippocampal synapses. J Neurosci 24:2380–2393.

Elmariah SB, Oh EJ, Hughes EG, Balice-Gordon RJ. 2005. Astrocytes regulate inhibitory synapse formation via Trk-mediated modulation of postsynaptic $GABA_A$ receptors. J Neurosci 25:3638–3650.

Erlander MG, Tillakaratne NJ, Feldblum S, Patel N, Tobin AJ. 1991. Two genes encode distinct glutamate decarboxylases. Neuron 7:91–100.

Essrich C, Lorez M, Benson JA, Fritschy JM, Luscher B. 1998. Postsynaptic clustering of major $GABA_A$ receptor subtypes requires the γ2 subunit and gephyrin. Nat Neurosci 1:563–571.

Fletcher TL, Cameron P, De Camilli P, Banker G. 1991. The distribution of synapsin I and synaptophysin in hippocampal neurons developing in culture. J Neurosci 11:1617–1626.

Goda Y, Davis GW. 2003. Mechanisms of synapse assembly and disassembly. Neuron 40:243–264.

Goldstein PA, Elsen FP, Ying SW, Ferguson C, Homanics GE, Harrison NL. 2002. Prolongation of hippocampal miniature inhibitory postsynaptic currents in mice lacking the $GABA_A$ receptor α1 subunit. J Neurophysiol 88:3208–3217.

Goslin K, Asmussen H, Banker G. 1998. Rat hippocampal neurons in low-density culture. In: Culturing nerve cells. Cambridge, MA: MIT Press. p 339–370.

Guastella J, Nelson N, Nelson H, Czyzyk L, Keynan S, Miedel MC, Davidson N, Lester HA, Kanner BI. 1990. Cloning and expression of a rat brain GABA transporter. Science 249:1303–1306.

Hamill OP, Marty A, Neher E, Sakmann B, Sigworth FJ. 1981. Improved patch-clamp techniques for high-resolution current recording from cells and cell-free membrane patches. Pflugers Arch 391:85–100.

Hutcheon B, Fritschy JM, Poulter MO. 2004. Organization of GABA receptor α-subunit clustering in the developing rat neocortex and hippocampus. Eur J Neurosci 19:2475–2487.

Ikegaki N, Saito N, Hashima M, Tanaka C. 1994. Production of specific antibodies against GABA transporter subtypes (GAT1, GAT2, GAT3) and their application to immunocytochemistry. Brain Res Mol Brain Res 26:47–54.

Isaacson JS, Solis JM, Nicoll RA. 1993. Local and diffuse synaptic actions of GABA in the hippocampus. Neuron 10:165–175.

Jensen K, Chiu CS, Sokolova I, Lester HA, Mody I. 2003. GABA transporter-1 (GAT1)-deficient mice: differential tonic activation of $GABA_A$ vs. $GABA_B$ receptors in the hippocampus. J Neurophysiol 90:2690–2701.

Johnston D, Wu SM-S. 1995. Foundations of cellular neurophysiology. Cambridge, MA: MIT Press.

Juttner R, Meier J, Grantyn R. 2001. Slow IPSC kinetics, low levels of alpha1 subunit expression and paired-pulse depression are distinct properties of neonatal inhibitory GABAergic synaptic connections in the mouse superior colliculus. Eur J Neurosci 13:2088–2098.

Kaufman DL, Houser CR, Tobin AJ. 1991. Two forms of the gamma-aminobutyric acid synthetic enzyme glutamate decarboxylase have distinct intraneuronal distributions and cofactor interactions. J Neurochem 56:720–723.

Kern W, Sieghart W. 1994. Polyclonal antibodies directed against an epitope specific for the α4-subunit of $GABA_A$ receptors identify a 67-kDa protein in rat brain membranes. J Neurochem 62:764–769.

Killisch I, Dotti CG, Laurie DJ, Luddens H, Seeburg PH. 1991. Expression patterns of $GABA_A$ receptor subtypes in developing hippocampal neurons. Neuron 7:927–936.

Laurie DJ, Wisden W, Seeburg PH. 1992. The distribution of thirteen $GABA_A$ receptor subunit mRNAs in the rat brain. III. Embryonic and postnatal development. J Neurosci 12:4151–4172.

Lavoie AM, Tingey JJ, Harrison NL, Pritchett DB, Twyman RE. 1997. Activation and deactivation rates of recombinant $GABA_A$ receptor channels are dependent on alpha-subunit isoform. Biophys J 73:2518–2526.

Li M, De Blas AL. 1997. Coexistence of two β subunit isoforms in the same gamma-aminobutyric acid type A receptor. J Biol Chem 272:16564–16569.

Liu QR, Lopez-Corcuera B, Mandiyan S, Nelson H, Nelson N. 1993. Molecular characterization of four pharmacologically distinct gamma-aminobutyric acid transporters in mouse brain [corrected]. J Biol Chem 268:2106–2112.

Mangan PS, Kapur J. 2004. Factors underlying bursting behavior in a network of cultured hippocampal neurons exposed to zero magnesium. J Neurophysiol 91:946–957.

Mangan PS, Sun C, Carpenter M, Goodkin HP, Sieghart W, Kapur J. 2005. Cultured hippocampal pyramidal neurons express two kinds of $GABA_A$ receptors. Mol Pharmacol 67:775–788.

McKernan RM, Whiting PJ. 1996. Which $GABA_A$-receptor subtypes really occur in the brain? Trends Neurosci 19:139–143.

Meier J. 2003. The enigma of transmitter-selective receptor accumulation at developing inhibitory synapses. Cell Tissue Res 311:271–276.

Mi R, Tang X, Sutter R, Xu D, Worley P, O'Brien RJ. 2002. Differing mechanisms for glutamate receptor aggregation on dendritic spines and shafts in cultured hippocampal neurons. J Neurosci 22:7606–7616.

Moss SJ, Smart TG. 2001. Constructing inhibitory synapses. Nat Rev Neurosci 2:240–250.

Mossier B, Togel M, Fuchs K, Sieghart W. 1994. Immunoaffinity purification of gamma-aminobutyric acidA ($GABA_A$) receptors containing γ1-subunits. Evidence for the presence of a single type of γ subunit in $GABA_A$ receptors. J Biol Chem 269:25777–25782.

Nusser Z, Mody I. 2002. Selective modulation of tonic and phasic inhibitions in dentate gyrus granule cells. J Neurophysiol 87:2624–2628.

Nusser Z, Sieghart W, Somogyi P. 1998. Segregation of different $GABA_A$ receptors to synaptic and extrasynaptic membranes of cerebellar granule cells. J Neurosci 18:1693–1703.

Okada M, Onodera K, Van Renterghem C, Sieghart W, Takahashi T. 2000. Functional correlation of $GABA_A$ receptor alpha subunits expression with the properties of IPSCs in the developing thalamus. J Neurosci 20:2202–2208.

Overstreet LS, Westbrook GL. 2003. Synapse density regulates independence at unitary inhibitory synapses. J Neurosci 23:2618–2626.

Owens DF, Liu X, Kriegstein AR. 1999. Changing properties of $GABA_A$ receptor-mediated signaling during early neocortical development. J Neurophysiol 82:570–583.

Peng Z, Hauer B, Mihalek RM, Homanics GE, Sieghart W, Olsen RW, Houser CR. 2002. $GABA_A$ receptor changes in δ subunit-deficient mice: altered expression of α4 and γ2 subunits in the forebrain. J Comp Neurol 446:179–197.

Poulter MO, Barker JL, O'Carroll AM, Lolait SJ, Mahan LC. 1992. Differential and transient expression of $GABA_A$ receptor α subunit mRNAs in the developing rat CNS. J Neurosci 12:2888–2900.

Poulter MO, Brown LA, Tynan S, Willick G, William R, McIntyre DC. 1999. Differential expression of α1, α2, α3, and α5 $GABA_A$ receptor subunits in seizure-prone and seizure-resistant rat models of temporal lobe epilepsy. J Neurosci 19:4654–4661.

Ramos B, Lopez-Tellez JF, Vela J, Baglietto-Vargas D, del Rio JC, Ruano D, Gutierrez A, Vitorica J. 2004. Expression of α5 $GABA_A$ receptor subunit in developing rat hippocampus. Brain Res Dev Brain Res 151:87–98.

Rao A, Cha EM, Craig AM. 2000. Mismatched appositions of presynaptic and postsynaptic components in isolated hippocampal neurons. J Neurosci 20:8344–8353.

Ribak CE, Tong WM, Brecha NC. 1996. GABA plasma membrane transporters, GAT-1 and GAT-3, display different distributions in the rat hippocampus. J Comp Neurol 1996 367:595–606.

Rivera C, Voipio J, Payne JA, Ruusuvuori E, Lahtinen H, Lamsa K, Pirvola U, Saarma M, Kaila K. 1999. The K^+/Cl^- co-transporter KCC2 renders GABA hyperpolarizing during neuronal maturation. Nature 397:251–255.

Roepstorff A, Lambert JD. 1992. Comparison of the effect of the GABA uptake blockers, tiagabine and nipecotic acid, on inhibitory synaptic efficacy in hippocampal CA1 neurones. Neurosci Lett 146:131–134.

Roepstorff A, Lambert JD. 1994. Factors contributing to the decay of the stimulus-evoked IPSC in rat hippocampal CA1 neurons. J Neurophysiol 72:2911–2926.

Sanes DH. 1993. The development of synaptic function and integration in the central auditory system. J Neurosci 13:2627–2637.

Sanes DH, Reh TA, Harris WA. 2000. Development of the nervous system. New York: Academic Press.

Sanes JR, Lichtman JW. 2001. Induction, assembly, maturation and maintenance of a postsynaptic apparatus. Nat Rev Neurosci 2:791–805.

Sara Y, Virmani T, Deak F, Liu X, Kavalali ET. 2005. An isolated pool of vesicles recycles at rest and drives spontaneous neurotransmission. Neuron 45:563–573.

Saxena NC, Macdonald RL. 1994. Assembly of $GABA_A$ receptor subunits: role of the delta subunit. J Neurosci 14:7077–7086.

Scotti AL, Reuter H. 2001. Synaptic and extrasynaptic gamma-aminobutyric acid type A receptor clusters in rat hippocampal cultures during development. Proc Natl Acad Sci U S A 98:3489–3494.

Serafini R, Ma W, Maric D, Maric I, Lahjouji F, Sieghart W, Barker JL. 1998. Initially expressed early rat embryonic $GABA_A$ receptor Cl^- ion channels exhibit heterogeneous channel properties. Eur J Neurosci 10:1771–1783.

Sieghart W, Sperk G. 2002. Subunit composition, distribution and function of $GABA_A$ receptor subtypes. Curr Top Med Chem 2:795–816.

Sieghart W, Item C, Buchstaller A, Fuchs K, Hoger H, Adamiker D. 1993. Evidence for the existence of differential O-glycosylated alpha 5-subunits of the gamma-aminobutyric acid A receptor in the rat brain. J Neurochem 60:93–98.

Sigworth FJ. 1981. Covariance of nonstationary sodium current fluctuations at the node of Ranvier. Biophys J 34:111–133.

Sipila S, Huttu K, Voipio J, Kaila K. 2004. GABA uptake via GABA transporter-1 modulates GABAergic transmission in the immature hippocampus. J Neurosci 24:5877–5880.

Sperk G, Schwarzer C, Tsunashima K, Fuchs K, Sieghart W. 1997. $GABA_A$ receptor subunits in the rat hippocampus I: immunocytochemical distribution of 13 subunits. Neuroscience 80:987–1000.

Sun C, Sieghart W, Kapur J. 2004. Distribution of α1, α4, γ2, and δ subunits of $GABA_A$ receptors in hippocampal granule cells. Brain Res 1029:207–216.

Swanwick CC, Harrison MB, Kapur J. 2004. Synaptic and extrasynaptic localization of brain-derived neurotrophic factor and the tyrosine kinase B receptor in cultured hippocampal neurons. J Comp Neurol 478:405–417.

Thompson SM, Gahwiler BH. 1992. Effects of the GABA uptake inhibitor tiagabine on inhibitory synaptic potentials in rat hippocampal slice cultures. J Neurophysiol 67:1698–1701.

Tia S, Wang JF, Kotchabhakdi N, Vicini S. 1996. Developmental changes of inhibitory synaptic currents in cerebellar granule neurons: role of $GABA_A$ receptor α6 subunit. J Neurosci 16:3630–3640.

Togel M, Mossier B, Fuchs K, Sieghart W. 1994. γ-Aminobutyric acid A receptors displaying association of γ3 subunits with β2/3 and different α subunits exhibit unique pharmacological properties. J Biol Chem 269:12993–12998.

Vicini S, Ferguson C, Prybylowski K, Kralic J, Morrow AL, Homanics GE. 2001. $GABA_A$ receptor α1 subunit deletion prevents developmental changes of inhibitory synaptic currents in cerebellar neurons. J Neurosci 21:3009–3016.

Vitellaro-Zuccarello L, Calvaresi N, De Biasi S. 2003. Expression of GABA transporters, GAT-1 and GAT-3, in the cerebral cortex and thalamus of the rat during postnatal development. Cell Tissue Res 313:245–257.